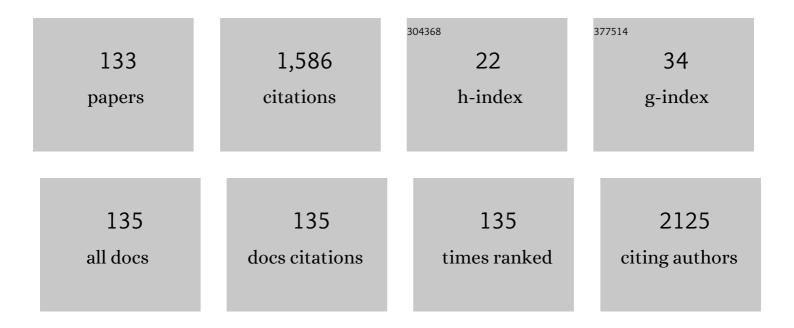
List of Publications by Year in descending order

Source: https://exaly.com/author-pdf/3335517/publications.pdf Version: 2024-02-01



LEANDRO L RANIERO

#	Article	IF	CITATIONS
1	Highly stable transparent and conducting gallium-doped zinc oxide thin films for photovoltaic applications. Solar Energy Materials and Solar Cells, 2008, 92, 1605-1610.	3.0	151
2	Role of hydrogen plasma on electrical and optical properties of ZGO, ITO and IZO transparent and conductive coatings. Thin Solid Films, 2006, 511-512, 295-298.	0.8	87
3	Role of annealing environment on the performances of large area ITO films produced by rf magnetron sputtering. Thin Solid Films, 2005, 487, 271-276.	0.8	63
4	Nanostructured silicon and its application to solar cells, position sensors and thin film transistors. Philosophical Magazine, 2009, 89, 2699-2721.	0.7	53
5	Salivary molecular spectroscopy: A sustainable, rapid and non-invasive monitoring tool for diabetes mellitus during insulin treatment. PLoS ONE, 2020, 15, e0223461.	1.1	47
6	Crystallization of amorphous indium zinc oxide thin films produced by radio-frequency magnetron sputtering. Thin Solid Films, 2008, 516, 1374-1376.	0.8	44
7	Amorphous/nanocrystalline silicon biosensor for the specific identification of unamplified nucleic acid sequences using gold nanoparticle probes. Applied Physics Letters, 2007, 90, 023903.	1.5	42
8	Analysis of saliva by Fourier transform infrared spectroscopy for diagnosis of physiological stress in athletes. Research on Biomedical Engineering, 2015, 31, 116-124.	1.5	41
9	High-wavenumber FT-Raman spectroscopy for in vivo and ex vivo measurements of breast cancer. Theoretical Chemistry Accounts, 2011, 130, 1231-1238.	0.5	39
10	Biofilm formation by Candida albicans is inhibited by photodynamic antimicrobial chemotherapy (PACT), using chlorin e6: increase in both ROS production and membrane permeability. Lasers in Medical Science, 2018, 33, 647-653.	1.0	38
11	Nanoparticles of methylene blue enhance photodynamic therapy. Photodiagnosis and Photodynamic Therapy, 2018, 23, 212-217.	1.3	36
12	Raman spectroscopy study of breast disease. Theoretical Chemistry Accounts, 2010, 125, 329-334.	0.5	33
13	In vitro evaluation of photodynamic therapy using curcumin on Leishmania major and Leishmania braziliensis. Lasers in Medical Science, 2016, 31, 883-890.	1.0	31
14	Synthesis and characterization of gold nanostructured Chorin e6 for Photodynamic Therapy. Photodiagnosis and Photodynamic Therapy, 2017, 18, 6-11.	1.3	31
15	DFT: B3LYP/6-311G (d, p) vibrational analysis of bis-(diethyldithiocarbamate)zinc (II) and natural bond orbitals. Spectrochimica Acta - Part A: Molecular and Biomolecular Spectroscopy, 2013, 105, 251-258.	2.0	29
16	Study of nanostructured/amorphous silicon solar cell by impedance spectroscopy technique. Journal of Non-Crystalline Solids, 2006, 352, 1880-1883.	1.5	28
17	Evaluation of methylene blue as photosensitizer in promastigotes of Leishmania major and Leishmania braziliensis. Photodiagnosis and Photodynamic Therapy, 2017, 18, 325-330.	1.3	27
18	Surface enhanced Raman scattering, electronic spectrum, natural bond orbital, and mulliken charge distribution in the normal modes of diethyldithiocarbamate copper (II) complex, [Cu(DDTC)2]. Spectrochimica Acta - Part A: Molecular and Biomolecular Spectroscopy, 2013, 116, 546-555.	2.0	26

#	Article	IF	CITATIONS
19	In and ex vivo breast disease study by Raman spectroscopy. Theoretical Chemistry Accounts, 2011, 130, 1239-1247.	0.5	24
20	Amniotic membrane as an option for treatment of acute Achilles tendon injury in rats. Acta Cirurgica Brasileira, 2017, 32, 125-139.	0.3	24
21	FT-IR characterization of a theranostic nanoprobe for photodynamic therapy and epidermal growth factor receptor targets. Sensors and Actuators B: Chemical, 2017, 240, 903-908.	4.0	23
22	Raman Spectroscopic Investigation of the Effects of Cosmetic Formulations on the Constituents and Properties of Human Skin. Photomedicine and Laser Surgery, 2012, 30, 85-91.	2.1	22
23	Development of a sensitive, stable and EGFRâ€specific molecular imaging agent for surface enhanced Raman spectroscopy. Journal of Raman Spectroscopy, 2015, 46, 434-446.	1.2	22
24	Chlorin e6-EGF conjugated gold nanoparticles as a nanomedicine based therapeutic agent for triple negative breast cancer. Photodiagnosis and Photodynamic Therapy, 2021, 33, 102186.	1.3	22
25	Role of buffer layer on the performances of amorphous silicon solar cells with incorporated nanoparticles produced by plasma enhanced chemical vapor deposition at 27.12 MHz. Thin Solid Films, 2005, 487, 170-173.	0.8	21
26	Magnetic particle imaging performance of liposomes encapsulating iron oxide nanoparticles. Journal of Magnetism and Magnetic Materials, 2020, 504, 166675.	1.0	21
27	Characterization of silicon carbide thin films prepared by VHF-PECVD technology. Journal of Non-Crystalline Solids, 2004, 338-340, 530-533.	1.5	20
28	Fourier Transform Infrared and Raman spectra, DFT: B3LYP/6-311G(d, p) calculations and structural properties of bis(diethyldithiocarbamate)copper(II). Spectrochimica Acta - Part A: Molecular and Biomolecular Spectroscopy, 2013, 105, 259-266.	2.0	20
29	Chlorin E6 phototoxicity in L. major and L. braziliensis promastigotes—In vitro study. Photodiagnosis and Photodynamic Therapy, 2016, 15, 19-24.	1.3	20
30	Photoconductivity activation in PbS thin films grown at room temperature by chemical bath deposition. Physica B: Condensed Matter, 2010, 405, 1283-1286.	1.3	19
31	Confocal Raman spectroscopy: determination of natural moisturizing factor profile related to skin hydration. Revista Brasileira De Engenharia Biomedica, 2014, 30, 11-16.	0.3	19
32	Silicon thin films prepared in the transition region and their use in solar cells. Solar Energy Materials and Solar Cells, 2006, 90, 3001-3008.	3.0	17
33	A Rheumatoid arthritis study using Raman spectroscopy. Theoretical Chemistry Accounts, 2011, 130, 1211-1220.	0.5	17
34	Overview of the use of theory to understand infrared and Raman spectra and images of biomolecules: colorectal cancer as an example. Theoretical Chemistry Accounts, 2011, 130, 1261-1273.	0.5	16
35	Characterization of Paracoccidioides brasiliensis by FT-IR spectroscopy and nanotechnology. Spectrochimica Acta - Part A: Molecular and Biomolecular Spectroscopy, 2016, 152, 397-403.	2.0	16
36	Finding reduced Raman spectroscopy fingerprint of skin samples for melanoma diagnosis through machine learning. Artificial Intelligence in Medicine, 2021, 120, 102161.	3.8	16

#	Article	lF	CITATIONS
37	Surface enhanced Raman scattering, electronic spectrum and Mulliken charge distribution in the normal modes of bis(diethyldithiocarbamate)zinc(II) complex. Spectrochimica Acta - Part A: Molecular and Biomolecular Spectroscopy, 2013, 110, 443-449.	2.0	15
38	Surface enhancement Raman scattering of tautomeric thiobarbituric acid. Natural bond orbitals and B3LYP/6-311+G (d, p) assignments of the Fourier Infrared and Fourier Raman Spectra. Spectrochimica Acta - Part A: Molecular and Biomolecular Spectroscopy, 2013, 114, 475-485.	2.0	15
39	In vivo Raman spectroscopy of breast tumors prephotodynamic and postphotodynamic therapy. Journal of Raman Spectroscopy, 2018, 49, 786-791.	1.2	15
40	Salivary Cortisol Responses and Session Ratings of Perceived Exertion to a Rugby Match and Fatigue Test. Perceptual and Motor Skills, 2017, 124, 649-661.	0.6	13
41	Study of nanostructured silicon by hydrogen evolution and its application in p–i–n solar cells. Journal of Non-Crystalline Solids, 2006, 352, 1945-1948.	1.5	12
42	Molecular structure, natural bond analysis, vibrational, and electronic spectra of aspartateguanidoacetatenickel(II), [Ni(Asp)(GAA)]·H2O: DFT quantum mechanical calculations. Spectrochimica Acta - Part A: Molecular and Biomolecular Spectroscopy, 2012, 97, 1041-1051.	2.0	12
43	Apoptosis-associated genes related to photodynamic therapy in breast carcinomas. Lasers in Medical Science, 2014, 29, 1429-1436.	1.0	12
44	Effect of gold oxide incorporation on electrochemical corrosion resistance of diamond-like carbon. Diamond and Related Materials, 2015, 53, 40-44.	1.8	12
45	Differentiation of Leishmania species by FT-IR spectroscopy. Spectrochimica Acta - Part A: Molecular and Biomolecular Spectroscopy, 2015, 142, 80-85.	2.0	12
46	Análise da composição bioquÃmica da pele por espectroscopia Raman. Revista Brasileira De Engenharia Biomedica, 2012, 28, 278-287.	0.3	11
47	Ribosomal DNA Nanoprobes studied by Fourier Transform Infrared spectroscopy. Spectrochimica Acta - Part A: Molecular and Biomolecular Spectroscopy, 2014, 118, 28-35.	2.0	10
48	The efficiency analysis of gold nanoprobes by FT-IR spectroscopy applied to the non-cross-linking colorimetric detection of Paracoccidioides brasiliensis. Sensors and Actuators B: Chemical, 2015, 215, 258-265.	4.0	10
49	FTIR study of secondary structure changes in Epidermal Growth Factor by gold nanoparticle conjugation. Biochimica Et Biophysica Acta - General Subjects, 2018, 1862, 495-500.	1.1	10
50	Characterization of the density of states of polymorphous silicon films produced at 13.56 and 27.12 MHz using CPM and SCLC techniques. Journal of Non-Crystalline Solids, 2004, 338-340, 206-210.	1.5	9
51	Electrical properties of amorphous and nanocrystalline hydrogenated silicon films obtained by impedance spectroscopy. Thin Solid Films, 2006, 511-512, 390-393.	0.8	9
52	In vitro apatite-forming ability of calcium aluminate blends. Ceramics International, 2017, 43, 10071-10079.	2.3	9
53	Characterization of optoelectronic platform using an amorphous/nanocrystalline silicon biosensor for the specific identification of nucleic acid sequences based on gold nanoparticle probes. Sensors and Actuators B: Chemical, 2008, 132, 508-511.	4.0	8
54	Identification of unamplified genomic DNA sequences using gold nanoparticle probes and a novel thin film photodetector. Journal of Non-Crystalline Solids, 2008, 354, 2580-2584.	1.5	8

#	Article	IF	CITATIONS
55	Photodithazine photodynamic effect on viability of 9L/lacZ gliosarcoma cell line. Lasers in Medical Science, 2017, 32, 1245-1252.	1.0	8
56	Evaluation of photodynamic therapy with methylene blue, by the Fourier Transform Infrared Spectroscopy (FT-IR) in Leishmania major - in vitro. Spectrochimica Acta - Part A: Molecular and Biomolecular Spectroscopy, 2019, 207, 229-235.	2.0	8
57	Surface properties of calcium aluminate cement blends for bone repair applications. Ceramics International, 2020, 46, 14241-14251.	2.3	8
58	Rapid identification of Paracoccidioides lutzii and P.ÂBrasiliensis using Fourier Transform Infrared spectroscopy. Journal of Molecular Structure, 2019, 1177, 152-159.	1.8	7
59	Molecular detection of HPV and FT-IR spectroscopy analysis in women with normal cervical cytology. Photodiagnosis and Photodynamic Therapy, 2020, 29, 101592.	1.3	7
60	Study of advanced rheumatoid arthritis. Revista Brasileira De Engenharia Biomedica, 2014, 30, 54-63.	0.3	7
61	Effect of the discharge frequency and impedance on the structural properties of polymorphous silicon. Thin Solid Films, 2004, 451-452, 264-268.	0.8	6
62	Multifunctional Thin Film Zinc Oxide Semiconductors: Application to Electronic Devices. Materials Science Forum, 2006, 514-516, 3-7.	0.3	6
63	Analysis of serum cortisol levels by Fourier Transform Infrared Spectroscopy for diagnosis of stress in athletes. Research on Biomedical Engineering, 2016, 32, 293-300.	1.5	6
64	Amorphous silicon-based PINIP structure for color sensor. Thin Solid Films, 2005, 487, 268-270.	0.8	5
65	Influence of the layer thickness and hydrogen dilution on electrical properties of large area amorphous silicon p–i–n solar cell. Solar Energy Materials and Solar Cells, 2005, 87, 349-355.	3.0	5
66	Identification of Paracoccidioides brasiliensis by gold nanoprobes. , 2012, , .		5
67	Phenylalanine ab initio models for the simulation of skin natural moisturizing factor. Spectrochimica Acta - Part A: Molecular and Biomolecular Spectroscopy, 2013, 106, 73-79.	2.0	5
68	FT-Raman spectroscopic study of skin wound healing in diabetic rats treated with Cenostigma macrophyllum Tul. Revista Brasileira De Engenharia Biomedica, 2014, 30, 47-53.	0.3	5
69	Epidermal Growth Factor Receptor–Specific Nanoprobe Biodistribution in Mouse Models. Journal of Pharmaceutical Sciences, 2016, 105, 25-30.	1.6	5
70	Improving the Radiopacity of Calcium Aluminate Cement Based Blends. Materials Research, 2018, 21, .	0.6	5
71	Synthesis of Iron Oxide Nanoparticles Optimized by Design of Experiments. Brazilian Journal of Physics, 2019, 49, 22-27.	0.7	5
72	Investigation of a-Si:H 1D MIS position sensitive detectors for application in 3D sensors. Journal of Non-Crystalline Solids, 2006, 352, 1787-1791.	1.5	4

#	Article	IF	CITATIONS
73	lsokinetic muscle performance and salivary immune-endocrine responses in handball players by Fourier transform infrared spectroscopy. Revista Andaluza De Medicina Del Deporte, 2017, 10, 125-131.	0.1	4
74	Calcium Aluminate Cement Blends Containing Bioactive Glass and Strontium for Biomaterial Applications. Materials Research, 2021, 24, .	0.6	4
75	Biochemical imaging of normal, adenoma, and colorectal adenocarcinoma tissues by Fourier transform infrared spectroscopy (FTIR) and morphological correlation by histopathological analysis: preliminary results. Research on Biomedical Engineering, 2015, 31, 10-18.	1.5	4
76	Impedance study of the electrical properties of poly-Si thin film transistors. Journal of Non-Crystalline Solids, 2006, 352, 1737-1740.	1.5	3
77	Performances of an in-line PECVD system used to produce amorphous and nanocrystalline silicon solar cells. Thin Solid Films, 2006, 511-512, 238-242.	0.8	3
78	Temperature influence on the thermal and structural properties of electrodeposited nanostructured black nickel cermet on high conductive C81100 copper. International Journal of Low-Carbon Technologies, 2011, 6, 86-92.	1.2	3
79	Application of FT-IR spectroscopy to assess physiological stress in rugby players during fatigue test. Research on Biomedical Engineering, 2016, 32, 123-128.	1.5	3
80	Tendinopathy diagnosis and treatment monitoring using attenuated total reflectanceâ€Fourier transform infrared spectroscopy. Journal of Biophotonics, 2018, 11, e201700256.	1.1	3
81	Using FT-IR spectroscopy for the identification of the T. cruzi, T. rangeli, and the L. chagasi species. Experimental Parasitology, 2018, 192, 46-51.	0.5	3
82	DIFFERENCES BETWEEN AMORPHOUS AND NANOSTRUCTURED SILICON FILMS AND THEIR APPLICATION IN SOLAR CELL. High Temperature Material Processes, 2007, 11, 575-583.	0.2	3
83	Specific nanomarkers fluorescence in vitro analysis for EGFR overexpressed cells in triple-negative breast cancer and malign glioblastoma. Photodiagnosis and Photodynamic Therapy, 2022, , 102997.	1.3	3
84	Characterization of silicon carbide thin films and their use in colour sensor. Solar Energy Materials and Solar Cells, 2005, 87, 343-348.	3.0	2
85	Insights on Amorphous Silicon Nip and MIS 3D Position Sensitive Detectors. Materials Science Forum, 2006, 514-516, 13-17.	0.3	2
86	Novel Optoelectronic Platform using an Amorphous/Nanocrystalline Silicon Biosensor for the Specific Identification of Unamplified Nucleic Acid Sequences Based on Gold Nanoparticle Probes. , 2007, , .		2
87	A rheumatoid arthritis study by Fourier transform infrared spectroscopy. Proceedings of SPIE, 2012, , .	0.8	2
88	Internalization of the PDZ and its photodynamic effect on the growth of ATCC and clinical strains ofE. coliandS. aureus. Laser Physics, 2016, 26, 095603.	0.6	2
89	Comparative Study of Morphometric and Fourier Transform Infrared Spectroscopy Analyses of the Collagen Fibers in the Repair Process of Cutaneous Lesions. Advances in Wound Care, 2016, 5, 55-64.	2.6	2
90	FTIR study of Achilles tendinopathy: protein secondary structure changes in tendon post injury. Research on Biomedical Engineering, 2018, 34, 350-355.	1.5	2

#	Article	IF	CITATIONS
91	Calcium aluminate cement-based blends for application to fill in bone defects. Research on Biomedical Engineering, 2020, 36, 429-438.	1.5	2
92	Compositions of calcium aluminate cement containing gold and silver nanoparticles for biomaterial applications. Research on Biomedical Engineering, 2020, 36, 139-146.	1.5	2
93	Triple-negative breast cancer treatment in xenograft models by bifunctional nanoprobes combined to photodynamic therapy. Photodiagnosis and Photodynamic Therapy, 2022, 38, 102796.	1.3	2
94	Composition, Structure and Optical Characteristics of Polymorphous Silicon Films Deposited by PECVD at 27.12 MHz. Materials Science Forum, 2004, 455-456, 100-103.	0.3	1
95	Growth of Polymorphous/Nanocrystalline Silicon Films Deposited by PECVD at 13.56 MHz. Materials Science Forum, 2004, 455-456, 532-535.	0.3	1
96	Batch Processing Method to Deposit a-Si:H Films by PECVD. Materials Science Forum, 2004, 455-456, 104-107.	0.3	1
97	Silicon Etching in CF ₄ /O ₂ and SF ₆ Atmospheres. Materials Science Forum, 2004, 455-456, 120-123.	0.3	1
98	Role of the rf frequency on the structure and composition of polymorphous silicon films. Journal of Non-Crystalline Solids, 2004, 338-340, 183-187.	1.5	1
99	Effect of the Load Resistance in the Linearity and Sensitivity of MIS Position Sensitive Detectors. Materials Research Society Symposia Proceedings, 2005, 862, 1561.	0.1	1
100	Study of a-SiC:H buffer layer on nc-Si/a-Si:H solar cells deposited by PECVD technique. , 0, , .		1
101	Role of Hydrogen Plasma on the Electrical and Optical Properties of Indium Zinc Transparent Conductive Oxide. Materials Science Forum, 2006, 514-516, 63-67.	0.3	1
102	Study of aggressiveness prediction of mammary adenocarcinoma by Raman spectroscopy. Proceedings of SPIE, 2012, , .	0.8	1
103	FTIR and SEM analysis applied in tissue engineering for root recovering surgery. Journal of Biomedical Materials Research - Part B Applied Biomaterials, 2017, 105, 1326-1329.	1.6	1
104	The comparison between label-free and non-cross-linking methods with gold nanoparticles for colorimetric detection of Paracoccidioides brasiliensis. Research on Biomedical Engineering, 2019, 35, 39-44.	1.5	1
105	Gold nanoparticles associated with temozolomide for glioblastoma Multiforme Treatment. Research, Society and Development, 2021, 10, e146101119406.	0.0	1
106	SPECTRAL RESPONSE OF LARGE AREA AMORPHOUS SILICON SOLAR CELLS. High Temperature Material Processes, 2004, 8, 293-299.	0.2	1
107	DNA Purifications Protocols for Fourier Transform Infrared Spectroscopy. , 2010, , .		1
108	Polymorphous Silicon Films Produced in Large Area Reactors by PECVD at 27.12 MHz and 13.56 MHz. Materials Research Society Symposia Proceedings, 2003, 762, 5131.	0.1	0

#	Article	IF	CITATIONS
109	Influence of the Rapid Thermal Annealing on the Properties of Thin a-Si Films. Materials Science Forum, 2004, 455-456, 108-111.	0.3	0
110	Role of Substrate on the Growth Process of Polycrystalline Silicon Thin Films by Low-Pressure Chemical Vapour Deposition. Materials Science Forum, 2004, 455-456, 112-115.	0.3	0
111	Sputtering Preparation of Silicon Nitride Thin Films for Gate Dielectric Applications. Materials Science Forum, 2004, 455-456, 69-72.	0.3	0
112	Optical and Morphological Properties of Annealed PbS Thin Films Obtained from a Chemical Solution Materials Science Forum, 2004, 455-456, 128-131.	0.3	0
113	MIS Photodiodes of Polymorphous Silicon Deposited at Higher Growth Rates by 27.12 MHz PECVD Discharge. Materials Science Forum, 2004, 455-456, 73-76.	0.3	0
114	Influence of Hydrogen plasma on electrical and optical properties of transparent conductive oxides Materials Research Society Symposia Proceedings, 2005, 862, 21101.	0.1	0
115	Amorphous Silicon Based p-i-i-n Structure for Color Sensor. Materials Research Society Symposia Proceedings, 2005, 862, 951.	0.1	0
116	Role of the Oxide Layer on the Performances of a-Si:H Schottky Structures Applied to PDS Fabrication. Materials Research Society Symposia Proceedings, 2006, 910, 4.	0.1	0
117	The Study of High Temperature Annealing of a-SiC:H Films. Materials Science Forum, 2006, 514-516, 18-22.	0.3	0
118	Evaluation of human serum of severe rheumatoid arthritis by confocal Raman spectroscopy. , 2010, , .		0
119	In vivo Raman spectroscopy of biochemical changes in human skin by cosmetic application. Proceedings of SPIE, 2010, , .	0.8	0
120	FT-IR microspectroscopy in rapid identification of bacteria in pure and mixed culture. Proceedings of SPIE, 2010, , .	0.8	0
121	Buccal microbiology analyzed by infrared spectroscopy. Proceedings of SPIE, 2012, , .	0.8	0
122	Biochemical differentiation of mycelium and yeast forms of Paracoccidioides brasiliensis by Fourier transform infrared spectroscopy. , 2012, , .		0
123	Phenylalanine gas phase and solvated models applied to skin NMF simulation by DFT calculations. Proceedings of SPIE, 2013, , .	0.8	0
124	DNA nanosensor surface grafting and salt dependence. Proceedings of SPIE, 2013, , .	0.8	0
125	EGFR-specific nanoprobe biodistribution in mouse models. Proceedings of SPIE, 2015, , .	0.8	0
126	Paracoccidioides brasiliensis Molecular Detection by the Label-Free Colorimetric Method Using Gold Nanoparticles. Brazilian Journal of Physics, 2019, 49, 55-61.	0.7	0

#	Article	IF	CITATIONS
127	Saliva diagnosis of autistic spectrum disorder by FT-IR spectroscopy. , 2021, , .		0
128	Biomarcadores plasmáticos e salivares para diagnóstico precoce de Transtorno do Espectro Autista: revisão sistemática. Research, Society and Development, 2021, 10, e412101018924.	0.0	0
129	Cancer Diagnosis by Optical Spectroscopy. , 2010, , .		0
130	The Determination of Biochemical Changes of Women Skin Layers as Function of Aging by Confocal Raman Spectroscopy. , 2010, , .		0
131	Abstract 250: Apoptosis-associated genes related to photodynamic therapy in breast carcinomas. , 2012, , .		0
132	DNA Surface Grafting and Gold Nanosensor. Sensor Letters, 2015, 13, 273-280.	0.4	0
133	INFLUÊNCIA DA CONCENTRAÇÃO DE OLIGONUCLEOTÃDEOS NO EFEITO DE AGLOMERAÇÃO DE NANOPARTÀULAS NA PRESENÇA DE SOLUÇÃO SALINA. Revista UniVap, 2016, 22, 126.	0.1	Ο